

Numerical Analysis and Testing of a New Segmented Brake Disc Fixed to the Wheel of a Wheelset

Wojciech SAWCZUK¹, Mateusz JÜNGST²

Summary

In electric multiple units due to the existence of the wheelsets, the brake discs are mounted on wheels of wheelsets. Although the braking of the vehicle is carried out mainly using an electrodynamic brake, depending on the type of braking implemented, a friction brake is additionally used in some braking phases. In the operation of driving wheelsets, the wear of the friction surface of the disc to the limit dimension occurs faster than the wear of the wheel rim. As a consequence, in the case of replacing full discs, it is necessary to squeeze the wheels from the axles of the wheelset, assemble the discs and press the wheels on the axle again. Squeezing and re-pressing the wheel due to the scratching of the axle surface is not possible to be repeated. For this reason, brake disc manufacturers offer split disks that enable their assembly without extrusion of the wheel from the axis of the wheelset. Thus, there is no need to roll the wheelset out of the trolley frame.

The article presents the construction of a new segment brake disc after testing on an inertia brake station for testing railway disc and block brakes based on Polish standards [2, 3]. With regard to the disc's construction itself, a new technology for its implementation has been proposed. Most brake discs are produced by casting and finishing machining. In the case of the proposed brake disc, the prototype of the disc was made by welding the venting elements with the disc's friction plate. The proposed brake disc was created during the implementation of the LIDER V project financed from the National Center for Research and Development in Warsaw.

Keywords: segmented brake disc, welding of the brake disc, bench tests

1. Introduction

In all rail vehicles with the exception of freight wagons, the disc brake is the basic (essential) friction brake (Figure 1). Only in traction vehicles (locomotives), in electric multiple units or in trams, the disc brake works with the electrodynamic brake (ED). Then, traction motors located near the driving wheelsets work like generators creating additional resistance, thus giving away part of the electric energy to the traction network to the traction network [5]. However, due to the low efficiency of the ED brake in the last braking phase, the disc brakes are operated pneumatically (PN) or electro-pneumatically (EP) at a speed of around 10 km/h. Depending on the braking implemented, e.g. during emergency braking, the friction brake can also be activated if the braking force of the electrodynamic brake is insufficient. The

simultaneous use of two brakes to increase the efficiency of the braking process is called “blending” [5]. This type of friction brake operation is also the cause of other operational problems occurring in the disc brake. Due to the short time of its operation (a few seconds), the friction pair of disc-cladding operates at much lower temperatures, which extends the break-in time of the linings against the disc and consequently reduces braking efficiency. Under the cladding, sediments (debris) are formed from the wear products and impurities present on the friction pair. In the case of stop brakes with only the disc brake, the friction lining is cleaned of dirt and consequently the larger surface is pressed against the brake disc. Therefore, at the stage of allowing the friction pair to be operated on a particular vehicle, additional tests are recommended at the brake station from the speed at which the disc brake will be operated.

¹ Ph.D. Eng.; Poznan University of Technology, Faculty of Transport Engineering, Institute of Combustion Engines and Transport, Department of Rail Vehicle; e-mail: wojciech.sawczuk@put.poznan.pl.

² M.Sc. Eng.; Poznan University of Technology, Faculty of Transport Engineering, Institute of Combustion Engines and Transport, Department of Rail Vehicle; e-mail: mateusz.m.jungst@doctorate.put.poznan.pl.

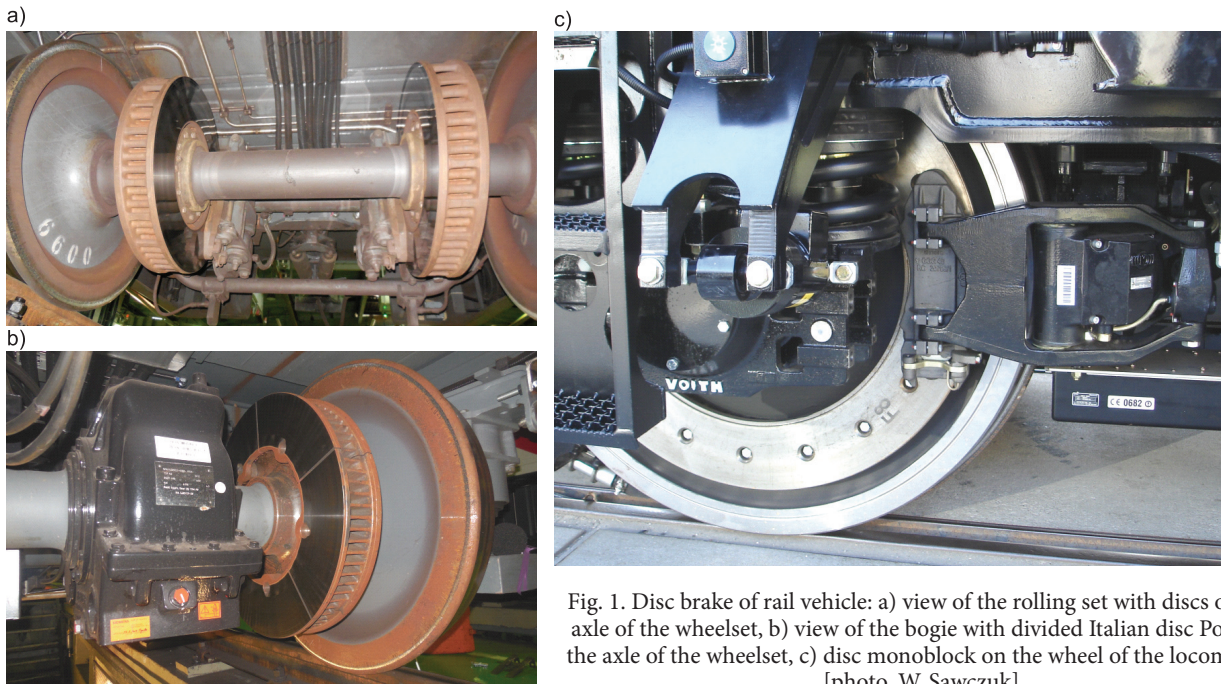


Fig. 1. Disc brake of rail vehicle: a) view of the rolling set with discs on the axle of the wheelset, b) view of the bogie with divided Italian disc Poly on the axle of the wheelset, c) disc monoblock on the wheel of the locomotive [photo. W. Sawczuk]

A separate issue related to brake discs for locomotives or electric multiple units is their faster wear relative to the rim (rim profile) of the wheels to which the discs are attached on both sides. As a consequence, it forces disassembly of the wheelset from the bogie frame and extrusion of the wheels from the axle. Due to the type of connection of the cold pressed wheel to the axle, this procedure cannot be repeatedly performed. Already at the stage of pressing in the wheel, the surface of the axle and the wheel seat are scratched. From the practice of repair shops repairing wheelsets, it is possible to squeeze the wheel twice from the wheelset axles to replace the full (monobloc) brake discs. At the next (third) replacement of the brake discs, it is necessary to purchase new wheels. To the extent of wear limit on the thickness of the friction surface (about 5 mm), the discs and the monobloc wheel rims are rolled on the underfloor lathes, which does not force the dismounting of the wheelset out of the trolley frame.

The purpose of the article is to present the concept of a segmented brake disc fixed to wheels of wheelsets after the first inertial tests with the program included in PN-EN 14535-3. The brake disc for tests has been made in the technology of welding friction plate with ventilation elements as opposed to cast discs.

2. Brake discs mounted on wheels of a wheelset

It is not always possible to attach the brake discs on the axle to rail vehicles with a drive wheelset due

to the installation of spaces between the wheels. In addition, the presence of traction motors in front of or behind the wheelset also in many rail vehicle constructions prevents the use of standard discs intended to be pressed onto the wheelset axle. Then it is necessary to attach the brake discs directly on the wheels, which is especially observed in the case of electric and diesel traction units as well as in locomotives. Wheel discs are divided into full (monolithic) wheels mainly found in rail vehicles as well as divided (segmented) for their assembly and disassembly in case of faster wear in relation to the wheel. Figure 2 shows some designs of brake discs for wheelset kits.

Most designs of brake discs mounted to the wheel are cast iron or steel castings with additional ventilation space. Due to the method of ventilation, discs with ventilating blades or rods are distinguished, as shown in Figure 3. In some designs of discs as shown in Figure 3c), there may also be venting blades and rods.

The choice of a given method of ventilation is determined by the designation of the brake disc. In the case of vehicles characterized by frequent stops, such as trains for passenger traffic, shields with ventilating blades are used, which are technologically easier to make with respect to discs with ventilating rods. For vehicles running at higher speeds above 160 km/h, bar ventilation is used due to lower ventilation losses relative to vane disks. In the case of high-speed vehicles, ventilation elements with an elliptical cross-section are set circumferentially, which greatly limits the flow of air flowing around the disc and thus reduces losses due to forced ventilation.

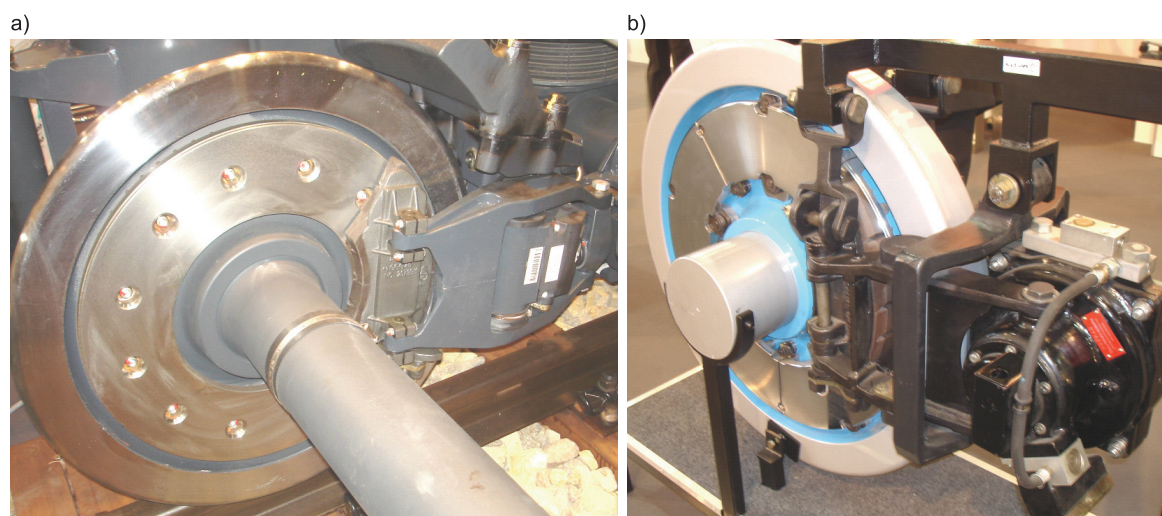


Fig. 2. Wheel brake discs: a) full (monolithic) for a rolling wheelset, b) split (segmented) Italian company Poli [photo. W. Sawczuk]

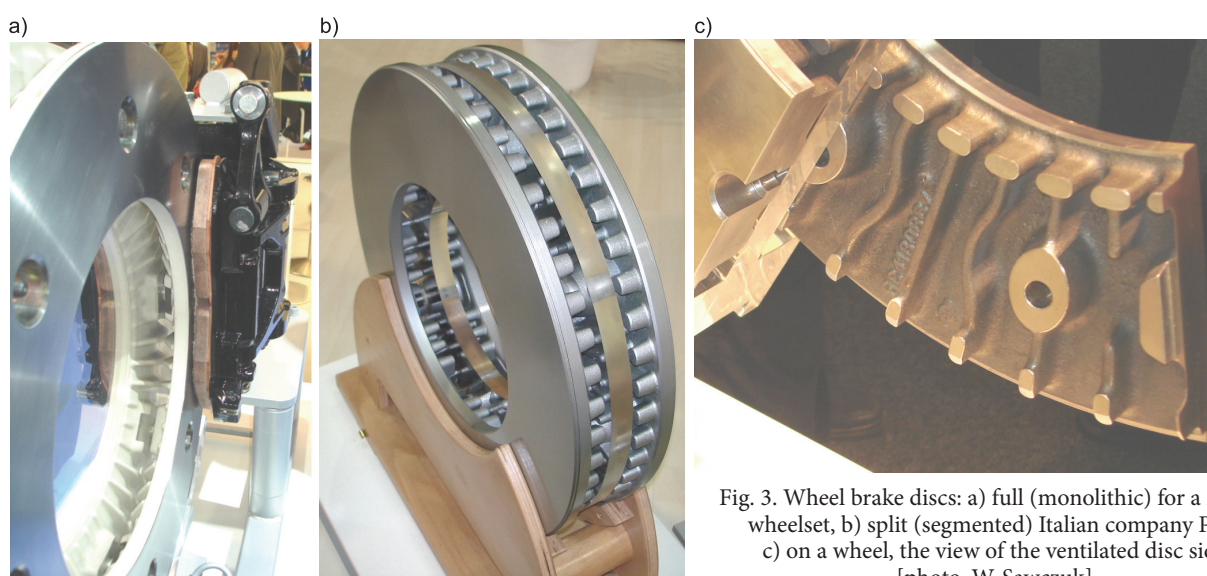


Fig. 3. Wheel brake discs: a) full (monolithic) for a rolling wheelset, b) split (segmented) Italian company Poli, c) on a wheel, the view of the ventilated disc side [photo. W. Sawczuk]

3. The concept of a new brake disc

The concept of a new segment disk based on three criteria was developed based on the literature on disc brake systems, their production method and information collected from the use of brake discs mounted to the wheel of a wheelset. The first technological criterion, the second construction criterion and the third criterion – exploitation criteria.

Ventilated disc brakes are in most cases steel or cast iron casts subjected to further finishing machining to the finished dimension. This is related to the mass production of brake discs and the number of disc castings is usually dictated by the capacity of the casting furnace in the case of casting a given batch. Due to the high cost

of the brake disc, orders from the manufacturer require a long waiting time and the ordering of a larger number of discs. It is very difficult to order single items, therefore, no inventory resources are created for orders of fewer brake discs. Figure 4 presents selected fragments from the production process of cast brake discs.

For this reason, in the new concept of the brake discs, it was proposed to produce by welding a friction ring made of a plate with circular fan elements.

The second criterion related to the construction of the disk assumes that it is segmented, divided into three segments. This is related to the possibility of disassembly damaged by surface cracks or exceeding the permissible limiting linear wear of the wheel disc without setting the wheelset from the bogie frame.



Fig. 4. View of selected stages from the production of segmented brake disc BK 141 mounted on the axle of the wheelset: a), b) view of castings of disc segments divided before machining, c) fixed disc segments on a lathe, d) view of segments on the table of a lathe with pre-machined friction surface, e) view of the brake hub with machined surfaces before drilling assembly holes with segments, f) assembly of segments to the brake hub by means of pins, g) view of the assembled two brake discs [photo. W. Sawczuk]

The third criterion concerning operation assumes the execution of a shield with independent segments. Then the assembly and disassembly of the wheel disc will be possible to be conducted by one employee of the technical back-up. Otherwise, the segmented disk, in which the individual parts are first combined with each other to obtain a friction ring and then, as an assembly fixed to the wheel disc, due to its weight (about 75 kg) require work of two people. In the case of a disc with independent segments, the employee assembles the parts directly on the wheel. The division into 3 segments weighing around 20–25 kg, on the one hand, makes it possible to perform assembly operations by one person as well as does not significantly affect the wear increase of the friction material at each wheel turn during braking, as shown in [1].

Figure 5 presents a view of two disc models, segmented with three segments and a full disc. For the full dial (produced by Kovis), there are 12 holes $\varnothing 32$ mm with chamfering 7 mm for M12 screws. The total length of the cutting edge is 555 mm for all mounting holes (Fig. 5a). In the case of segmented disk (Fig. 5b), it was proposed to divide it into three segments and abandon 6 holes for M12 bolts. Then, in places where the holes on the disc are abandoned, the screws are screwed into the threaded rods of the inner side of the disc on the other side of the wheel. In the proposed solution, through-holes for bolts secured at the ends by nuts are omitted. The M12 screws are screwed into the threaded holes of the segments on the other side of the wheel. When resigning from 6 holes for M12 screws (22 mm diameter with chamfering 2 mm) and

3 segments (3 cutting edges with a width of 145 mm), the total length of the cutting edge is 567 mm and is only 12 mm larger than the full disc. On this basis, it is stated that the 3-segment disc with non-bolt screws on the other side of the wheel will be characterized by a similar wear of friction material as the full disc.

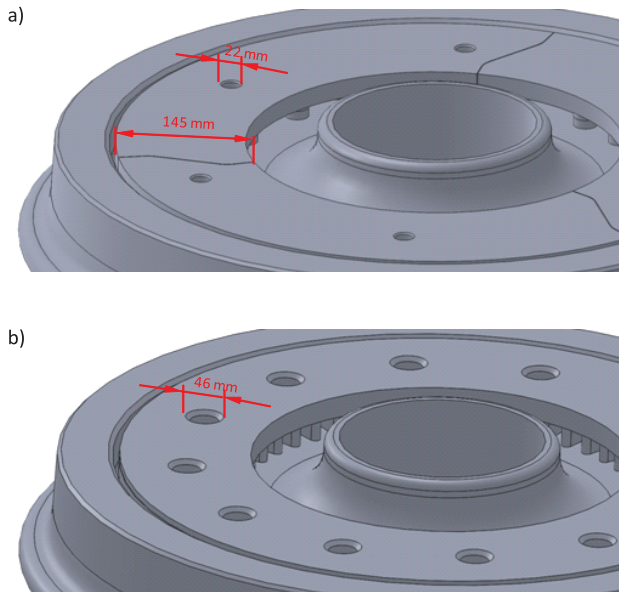


Fig. 5. View of the rings together with the width of the cutting edges affecting the wear of friction linings on the example of the wheel: a) monolithic (full), b) segment (split) [own study]

In the case of other manufacturers of split brake discs, the friction ring is divided into 2, 4, 5 and more segments depending on the diameter of the disc. However, it should be emphasized that the division of the disc into more than 3 segments will affect the significant increase in the wear of friction material, which is disadvantageous from the later use of the friction pair of the disc brake.

4. Numerical analysis of brake discs

The suggested segment brake disc before the prototype was made was modeled in the SolidWorks 2016 environment. Numerical analyzes were performed to determine the temperature distributions, stresses and disc deformations. The model of mounted segments on the wheel with respect to the monolithic (full) disk is shown in Figure 6.

Numerical analyzes were carried out for the case of braking the PESA Elf 22WE (EN76) traction unit from a speed of 160 km/h to a stop. The value of the heat flux acting on the blades during the braking procedure was calculated on the basis of the data in Table 1.

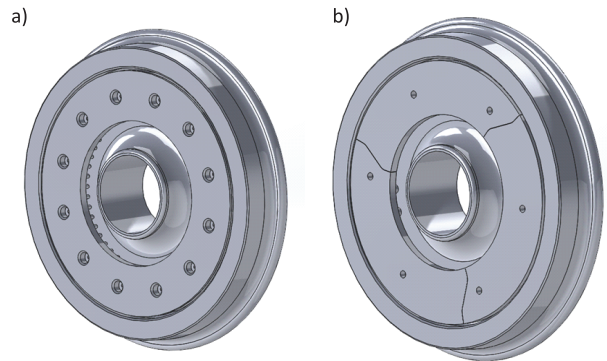


Fig. 6 – Wheel model made in the SolidWorks2016 environment: a) monolithic (full), b) segmented (split) without fixing bolts [own study]

Table 1

Data to calculate the heat flux acting on the surface of the brake disc [1]

Parameter	Value
Rail vehicle weight (EN76 22WE) – M [kg]	135000
Initial vehicle speed – v_0 [m/s]	44.4
Radius of the brake disk – r_d [m]	0.355
Radius of a rail vehicle wheel – r_w [m]	0.445
Braking time – t_s [s]	37'
Brake delay – a [m/s ²]	1.2
Distribution of brake force distribution – P	0.1
The outside diameter of the brake disc – D_z [m]	0.72
Inner diameter of the brake disc – D_w [m]	0.42

The braking force acting on the brake disc of the rail vehicle is determined from the potency (1) [6]:

$$F_{DISC} = \frac{\frac{1}{2} \cdot P \cdot M \cdot v_0^2}{2 \cdot \frac{r_d}{r_w} \cdot \left(v_0 \cdot t_z - \frac{1}{2} \cdot a \cdot t_z^2 \right)} = \frac{\frac{1}{2} \cdot 0.1 \cdot 135000 \cdot 44.4^2}{2 \cdot \frac{0.355}{0.455} \cdot \left(44.4 \cdot 37 - \frac{1}{2} \cdot 1.2 \cdot 37^2 \right)} = 10383.4 \text{ N} \quad (1)$$

The friction surface of the brake disc was calculated based on dependence (2):

$$A = \frac{\pi \cdot D_z^2}{4} - \frac{\pi \cdot D_w^2}{4} = 0.407 - 0.0139 = 0.269 \text{ m}^2 \quad (2)$$

The heat flow acting on one side of the target in accordance with [5] determines the dependence (3).

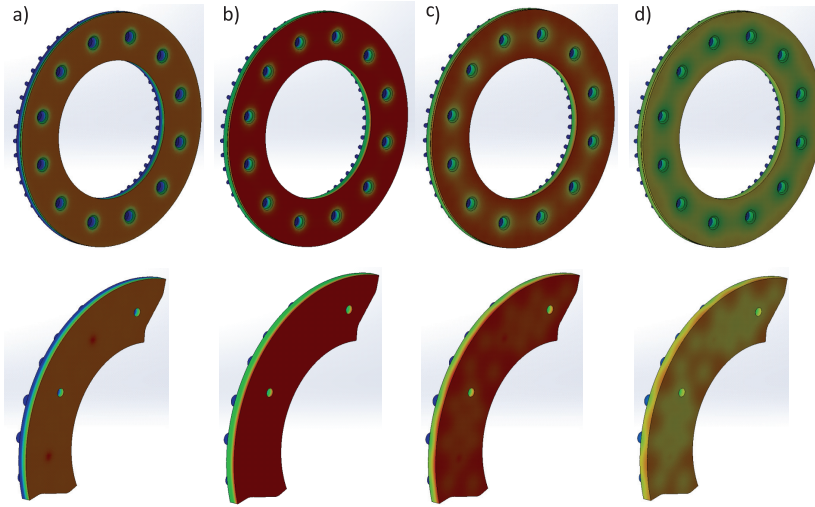


Fig. 7. Distribution of temperature on the full (unbranded) disc and segmented (split) disc after simulated braking lasting 37 seconds at the moment of time: a) 10 s, b) 20 s, c) 30 s, and d) 37 s [own study]

$$Q(t) = F_{disc} \cdot v_{disc}(t) = F_{disc} \cdot \frac{r_{disc}}{r_{wheel}} \cdot (v_0 - a \cdot t) = 359640 - 9720(t) \text{ W} \quad (3)$$

The density of the heat flux shows the dependence (4) [6]:

$$q = \frac{Q(t)}{A} = \frac{359640}{0,269} = 1338911,9 \frac{\text{W}}{\text{m}^2} \text{ dla } t=0 \text{ s} \quad (4)$$

Using the dependencies (1)–(4), numerical simulations of the temperature distribution on the brake discs were carried out during braking. Figure 7 shows the temperature distribution of the brake discs after stop braking simulation for selected time moments.

For each moment of braking after the simulation, the maximum temperature of the disc was determined. On this basis, the temperature characteristics of the discs (full and segmented) were generated during simulated braking lasting 37 seconds (Figure 8).

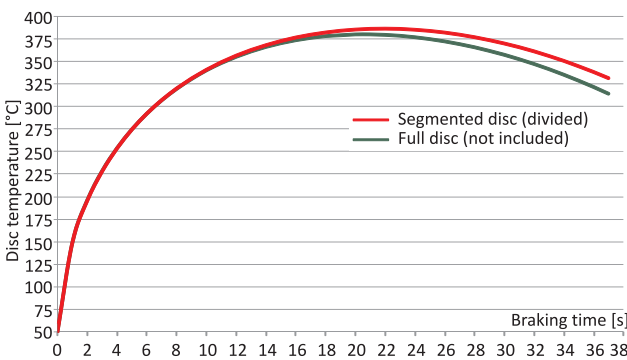


Fig. 8. Distribution of average temperature of brake discs after simulated emergency braking with speed $v = 160 \text{ km/h}$ [own study]

To determine the braking torque M_h acting on the disc during the dynamometer process, the mean value of the coefficient of friction of 0.35 required by the UIC 541-3 card was assumed. The braking torque was calculated using the dependence (5) [8]:

$$M_h = 2 \cdot \mu \cdot F_{disc} \cdot r_h = 2 \cdot 0.35 \cdot 10383.4 \cdot 0.285 = 2071.5 \text{ Nm} \quad (5)$$

Figure 9 shows the view of the brake discs with the Mises reduced stress distribution.

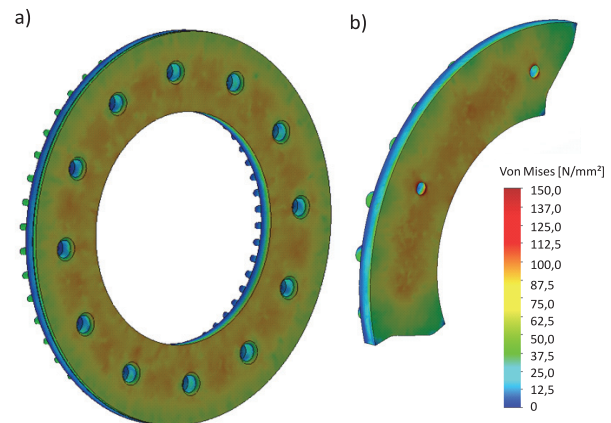


Fig. 9. Numerical analysis of von Mises reduced stresses for the disc a) standard (full), b) segmented (split) [own study]

In the simulation, the values of stresses were measured at four locations on the friction surface of the disc, i.e. on the outer radius, in the middle part without the mounting hole, in the middle part on the edge of the mounting hole and on the inner radius. internal. The results of the reduced stresses are summarized in the form of a bar graph in Figure 10.

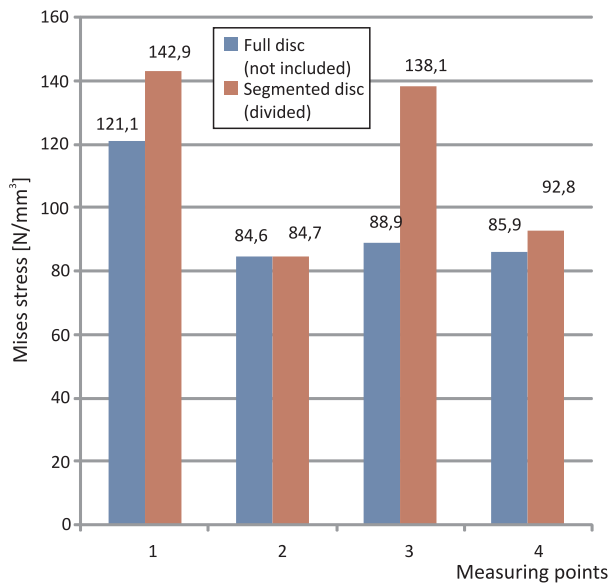


Fig. 10. Dependencies between reduced Mises stress from measuring points 1–4: 1) outer radius of the disc, 2) central part of the disc, 3) central part of the disc on the edge of the mounting hole, 4) inner radius of the disc [own study]

Analyzing the graph shown in Figure 10, it is stated that the greatest stress difference occurs in the middle part of the segment disk at the edge of the mounting hole relative to the full disk. This is related to the small dimension (2 mm) of the chamfering edge of the hole. In full discs there are chamfers at a depth of 5–7 mm, depending on the manufacturer. The chamfers on the holes on the one hand reduce stress on the edge, on the other hand, they increase the diameter of the hole at the friction surface, which extends the cutting edge and affects the higher consumption of friction material.

The next stage of numerical analyses was to check the displacements (deformations) of the brake discs as a result of the heat flux and the braking torque. The results are shown in Figure 11.

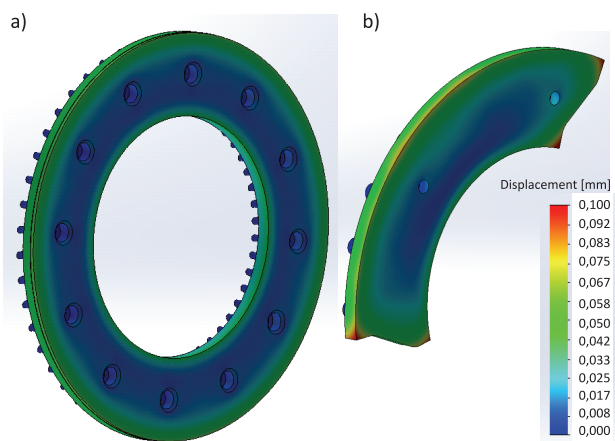


Fig. 11. View of displacement of the disc: a) full, b) segment [own study]

The list of maximum displacements (deformations) of the brake discs on the external and internal radius is shown in Figure 12. It should be emphasized that despite the higher performance in the case of a segment disk, deviations defined in PN-EN 14535-2 [3] are not exceeded.

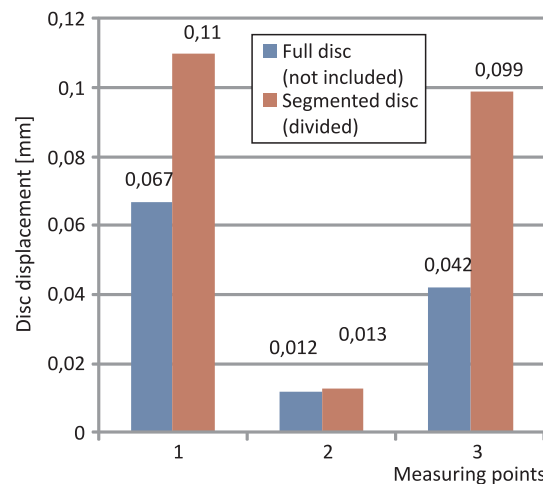


Fig. 12. Maximum displacement values on the external radius (1), in the middle part (2) and on the inner radius (3) of the brake discs [own study]

In both cases, the greatest deformations occur on the external radius and amount to 0.067 mm for the full disk and 0.11 for the segment disk respectively.

It should be emphasized that numerical analyses are indispensable in the process of designing braking system components before stationary or operational tests (prototype tests). In some cases, additionally numerical simulations are extended by analysis of air flow outside and inside the pole or fatigue analysis. The authors of the study [10] also undertook the task of simulating the life expectancy of the brake disc. The analysis of the propagation of a single crack formed in a macroscopic hot spot on a wheel-mounted disc, which subsequently increased the length and depth due to successive emergency braking, well correlated with the results of other studies indicating the elliptic shape of discontinuities in the friction ring. Figure 13 shows the distribution of peak temperatures achieved during emergency braking from a speed of 400 km/h.

It is stated that along with the propagation of the crack, the stresses in the rest of the friction ring decrease (Fig. 14)

The research has shown that the rate of crack propagation increases over time: the longer the crack is broken, the greater its increase at successive braking. From the point of view of railway applications, a very important publication is the study [9], focused on issues related to air flow in shield ventilation chan-

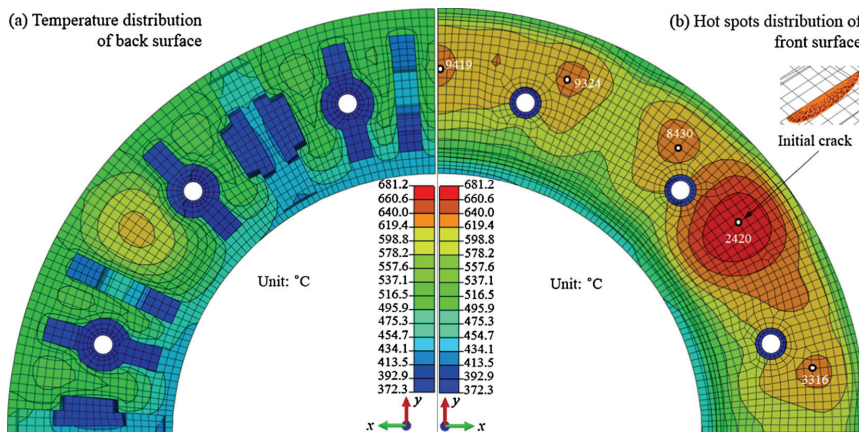


Fig. 13. Peak temperatures of the steel brake disc fixed to the wheel: a) the rear side of the friction ring, b) the front side of the friction ring [10]

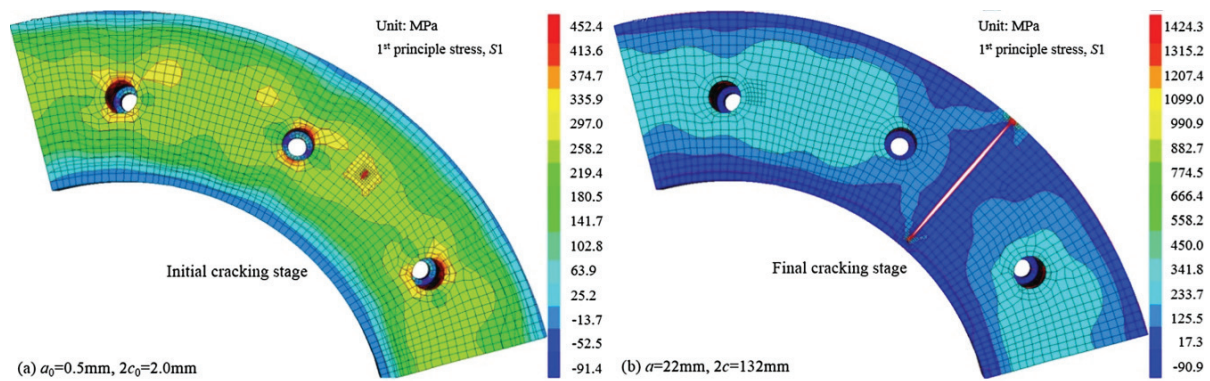


Fig. 14. Distribution of stresses in the friction ring of the brake disc: a) for an initial crack of 2 mm, b) for a maximum crack of 132 mm [10]

nels and the associated convective heat exchange. The authors undertook the development of a new disc constituting a synthesis of structural solutions of other discs for the railways: they applied a row of tangential blades and then shorter radial blades closer to the center of the disc. A few years after design and experimental tests, the three-dimensional shield model has been subjected to CFD analyzes. The simulation assumed rotation of the target in the medium in steady state (without air movement) at the speed of 1500 rpm.

Figure 15 shows the distribution of local convective heat transfer coefficient on blades and connectors for the disc heated to 200°C at 1500 rpm in fixed air at 20°C.

The results clearly indicated large local variability of the coefficient. The lowest values of approx. 7 W/m² K (corresponding to natural convection) were recorded in the booms – area b. The highest values of 118 W/m² K were recorded in areas with maximum flow velocity – area a. The importance of the total mean heat transfer coefficient should be emphasized, because this value multiplied by the total flowing area of the target determines the total convective output power (heat dissipation rate) used in the design calculations [9].

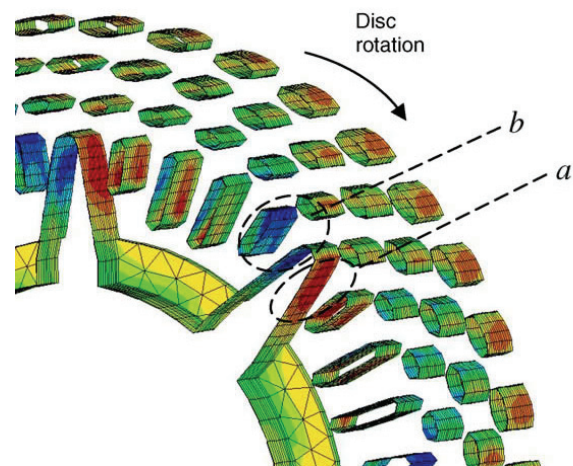


Fig. 15. Distribution of convective heat transfer coefficient in shield channels [9]

5. Execution of the brake disc prototype for bench tests

The individual segments of the brake disc for tests (6 pieces) were made of a 25 mm thick, laser-cut plate,

with a finishing allowance for external and internal diameter of the disk after assembly together with holes for venting, assembly and fixing rods.

After connecting the bars with the plate, the next operation was peripheral welding of the plates in beveling of the bars from the friction surface. In order to remove welding stresses, segments were subjected to stress relief annealing. Then, the final finishing treatment was performed on milling of the friction surface of the segments, the inner

surface of the segment contact with the wheel disk, and the holes for the fixing bolts and the mounting bolts. Figure 16 shows selected fragments in the construction of a prototype disk for friction-mechanical tests at the brake station.

The last stage before standby friction-mechanical tests was the assembly of 6 thermocouples in accordance with [3] 3 on each side of the target and the assembly of disc segments on the wheel. Figure 17 shows assembly of segments to the wheel disk in several stages.

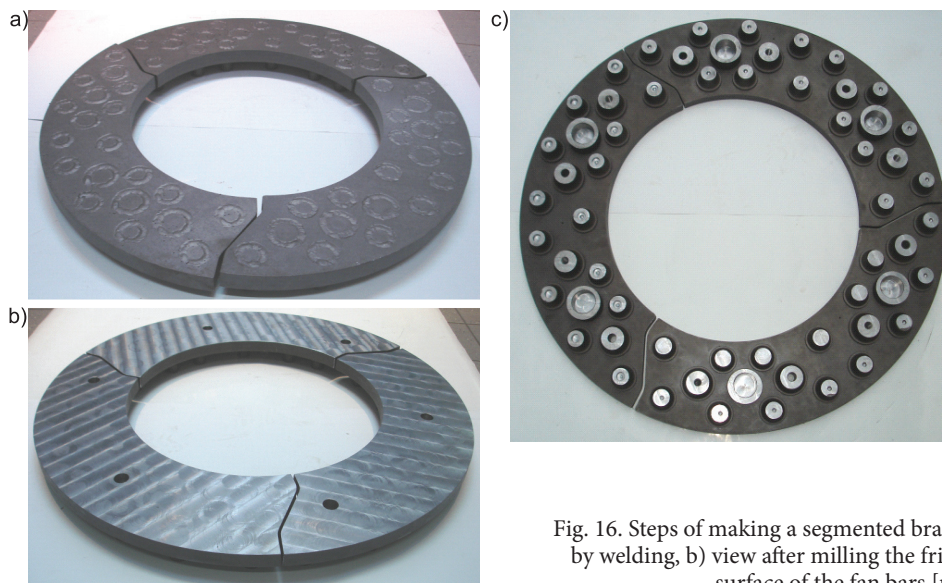


Fig. 16. Steps of making a segmented brake disc: a) connecting disc with rods by welding, b) view after milling the friction surface to size, c) milling the surface of the fan bars [photo. W. Sawczuk]



Fig. 17. Mounting of the segment disk to the wheel: a)–c) individual stages of assembly of the segments to the wheel, d) view of the wheel with mounted discs before assembly on the shaft of the brake station [photo. W. Sawczuk]

6. Methodology of brake discs testing

The friction-mechanical tests (where the change of coefficient of friction and the temperature of the disc during braking were recorded) were carried out at the Rail Vehicles Institute TABOR in Poznan on the inertia test stand for brake pads and disc rail vehicles. The test object was a segment disc with an outer diameter of 720 mm with ventilating rods mounted on the wheel. The shield formed a friction pair with Frenoplast 200 FR20H.2 organic pads.

The shield was tested in accordance with the guidelines included in the PN EN 14535-3 standard for the type B1 test class being the mapping of braking occurring in the electric traction unit as the EN 76 22Wea (Pesa Elf) vehicle. It is a 4-unit vehicle running at a maximum speed of 160 km/h with a length of 72.25 m and a service weight of 135 t [1]. The parameters of the brake disc qualification test for a given railway vehicle are presented in Table 1. On the maximum speed vehicle servo for which the target is tested, the mass to deceleration per one disc, using the entries in Table 2, it is possible to determine the occupational test class.

Next, the PN EN [4] standard specifies the braking tests procedure for reducing the speed of the vehicle on the basis of Table 2. The first 10 inhibitions for class B1 are made from 160 to 140 km/h while another 10 braking from speeds of 110 to 95 km/h. The entire test

program consists of 10 repetitions of a given program cycle, in accordance with Table 6 contained in [4]. The test of the blade strength in total consists of 1000 braking, to accelerate the occurrence of surface cracking on the brake disc during emergency braking from 160 km/h to 0, service brakes from a speed of 2/3 of the maximum speed to 0 and inhibitions from different speeds. The assumption of this test included in the standard [4] is to check the maximum effectiveness of the tested brake disc for the braking cases included in a given braking class.

Brake strength test is the first test carried out in accordance with PN EN 14535-3. Another test is the heat dissipation test, carried out as a constant power braking (simulation of the train descent from a hill in 30 minutes), centrifugal force test, energy loss test for ventilation of the brake disc during its rotation and a friction brake generated by the friction pair.

The data contained in Tables 1, 2 and 3 are necessary to enter the test procedure of the dynamometric position for testing the disk brake. Figure 18 shows the view of the test stand from the side of the tested brake disc with an attached lever mechanism.

7. Brake discs test results

During the tests in the inertial bench, the instantaneous pressure was applied to the brake discs and the

Table 2

Classification test parameters

Class	Maximum Energy of the class W_b [MJ]	Maximum Power of the class P_m [kW]	Class speed v_m [km/h]	Braked mass m [t]	Initial brake disc temperature Θ_0 [°C]	Deceleration rate a_m [m/s ²]
A1	4.6	400	120	10	50-60	1.2
B1	7.9	427	160	8	50-60	1.2
B2	9.9	533	160	10	50-60	1.2
C1	12.3	533	200	8	50-60	1.2
C2	15.4	667	200	10	50-60	1.2
D1	20.5	472	250	8.5	50-60	0.8
E1	27.8	533	300	8	50-60	0.8
F1	23.6	389	350	5	50-60	0.8
F2	28.4	467	350	6	50-60	0.8
F3	33.1	544	350	7	50-60	0.8
G1	37	533	400	6	50-60	0.8

[Own elaboration].

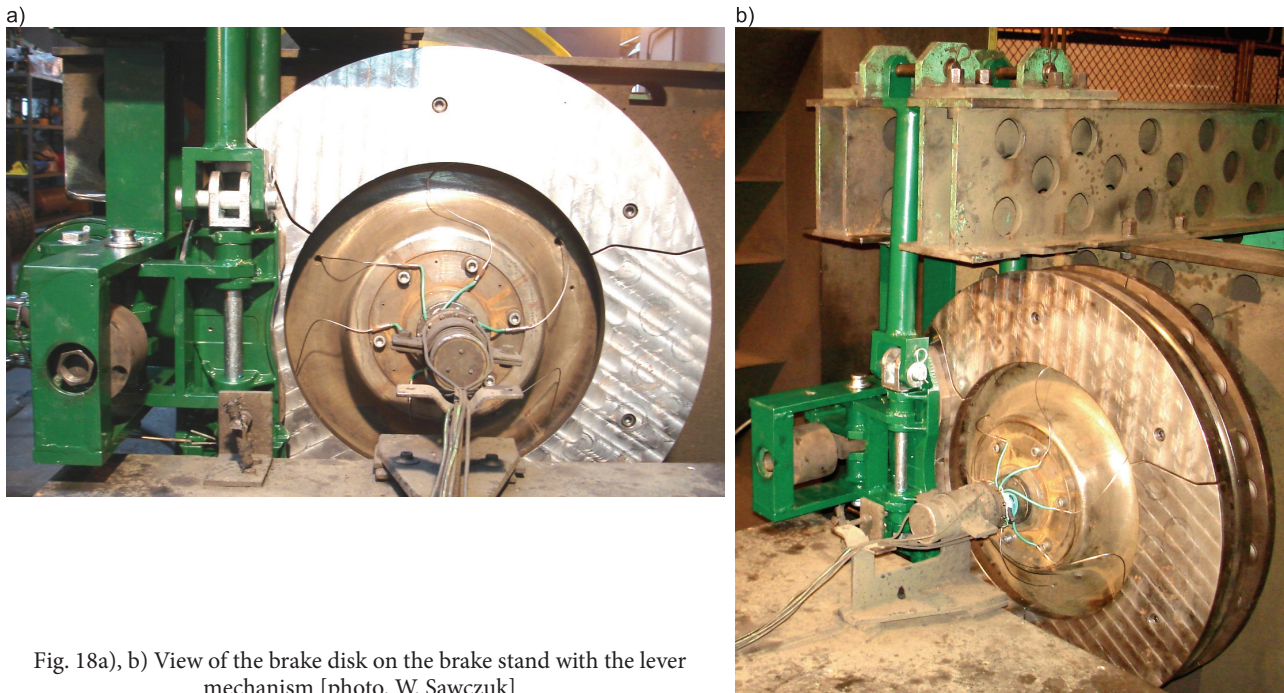


Fig. 18a), b) View of the brake disc on the brake stand with the lever mechanism [photo. W. Sawczuk]

tangent force related to the braking radius in order to determine the instantaneous coefficient of friction according to the relation (6) [2]:

$$\mu_a = \frac{F_t}{F_b} \quad (6)$$

where:

F_t – instantaneous tangent force relative to the braking radius r ,

F_b – total instantaneous contact pressure on the brake disc.

On the basis of the determined instantaneous coefficient of friction, the characteristics of changes of the braking torque are made and the average coefficient of friction is determined according to the relationship (7) as the integral of the instantaneous coefficient of friction along the braking path [2]:

$$\mu_m = \frac{1}{s_2} \int_0^{s_2} \mu_a ds \quad (7)$$

where: s_a – braking distances in meters.

On the basis of dependence (6) and (7), the characteristics $\mu_a = f(v)$ and $\mu_m = f(v)$ are determined. On this basis, the moment of reaching the maximum and minimum momentary coefficient of friction is determined. The results obtained from dependence

(7) are final summaries checking the coefficient of friction in the entire braking speed range of a given vehicle. The dependence of the instantaneous coefficient of friction on the speed for emergency braking and braking as well as service braking is shown in Figures 19–22.

The results of the instantaneous coefficient of friction shown in Figures 19–22 refer to the first 100 brakings. Figure 23 presents the values of the average coefficient of friction for braking and braking from various speeds. For the first 100 braking cycles, the value of μ_m with the standard deviation was determined based on the relationship (7) for brakes from 110 km/h (73 repetitions), 160 km/h (6 repetitions) and brakes from speeds of 140 to 95 km/h (10 repetitions) and from a speed of 160 to 110 km/h (11 repetitions). Additionally, on the basis of the UIC 541-3 leaflet, the tolerance of the average coefficient of friction is marked on the graph.

The results of the average temperature distribution obtained by the segmented brake disc are shown in Figure 24 for the brakings and braking tests.

When analyzing the graph of the average temperature of the brake disc for the first 100 brakings and braking tests, there was no over-cut of the disc of 400°C according to [2] due to the limitations of the organic friction material.

Table 3 presents the values of the weight consumption of one set of friction pads after 100 brakings. On one set of linings, it was possible to perform 300 brakes according to Standards [4].

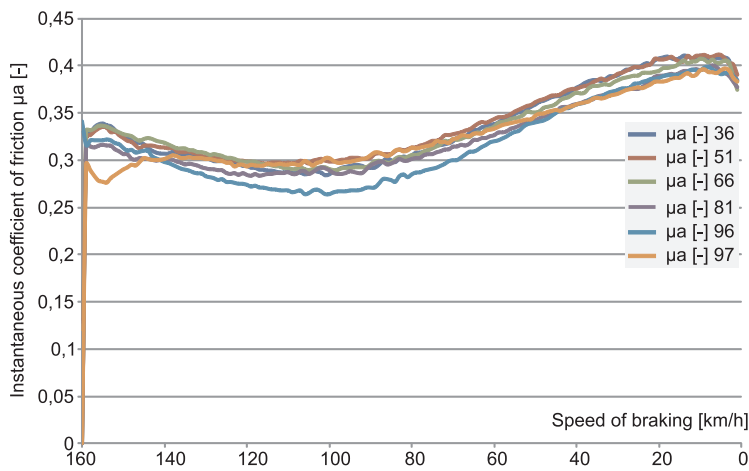


Fig. 19. Dependence of instantaneous coefficient of friction on speed during emergency braking from 160 km/h to 0 [own study]

Fig. 20. Dependence of the instantaneous coefficient of friction on the velocity of the braking speed from 160 to 110 km/h [own study]

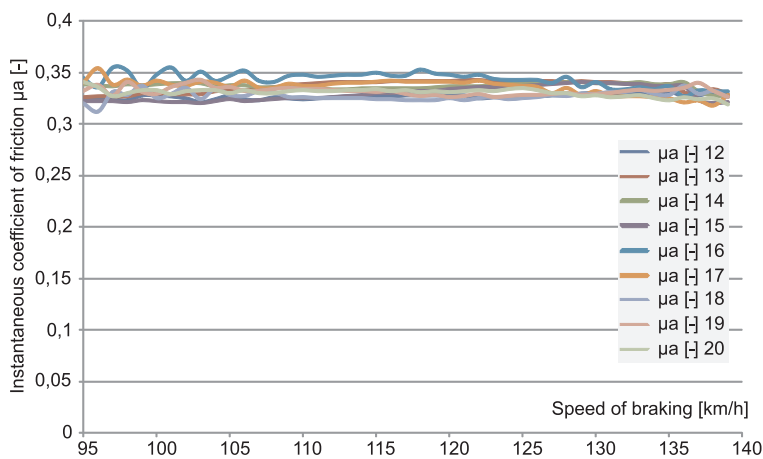
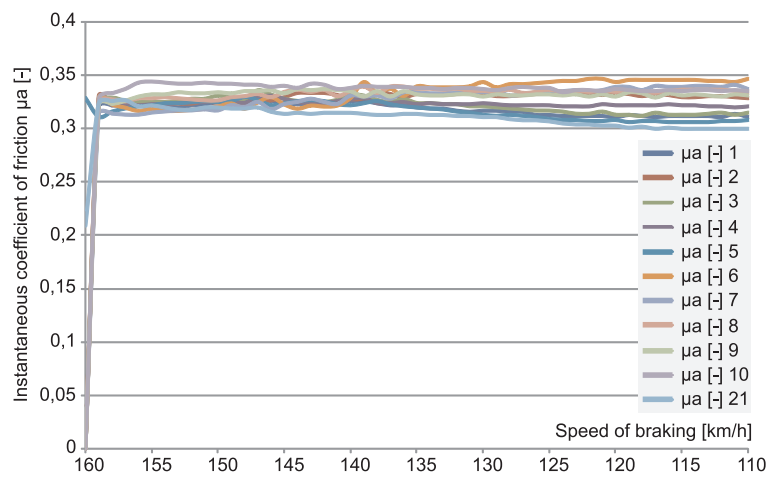


Fig. 21. Dependence of the instantaneous coefficient of friction on velocity over time of braking from speeds of 140 to 95 km/h [own study]

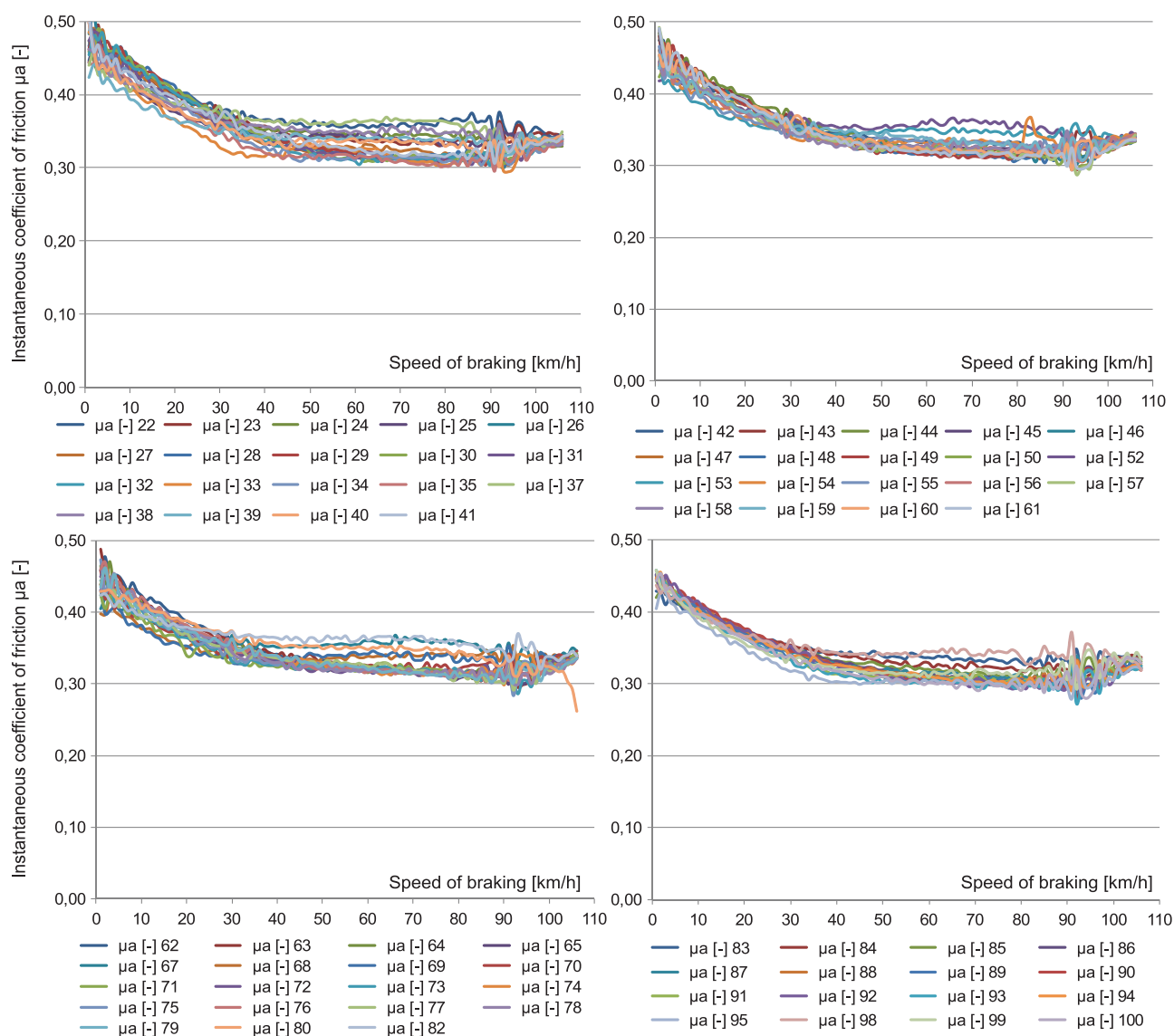


Fig. 22. Dependence of instantaneous coefficient of friction on speed during service braking from 110 km/h to 0, a), b), c), d) next series of brakes [own study]

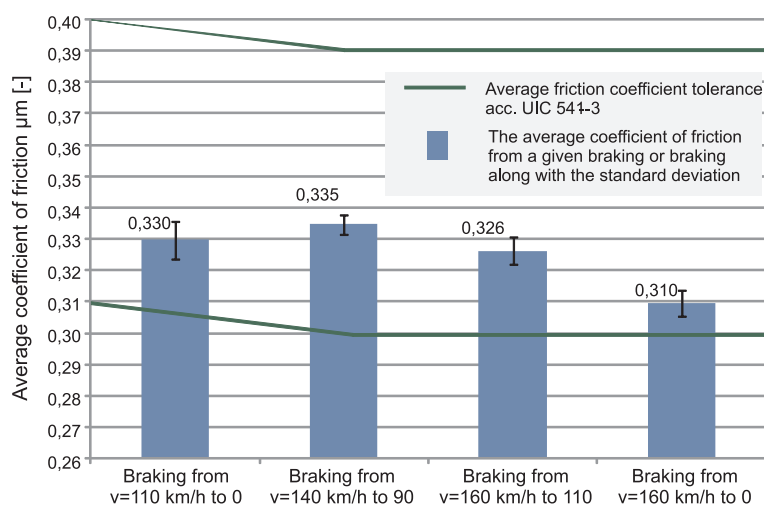


Fig. 23. Comparison of the average coefficient of friction obtained from various brakings and braking speeds in relation to the requirements of the UIC 541-3 leaflet [own study]

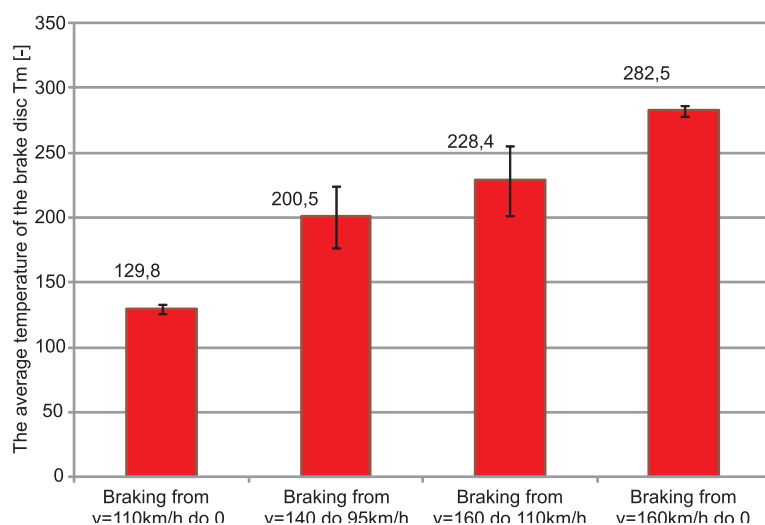


Fig. 24. Juxtaposition of the average temperature of the brake disc obtained from various brakings and braking speeds [own study]

Table 3

Mass (weight) wear of friction material

Page	Weight of pads after lapping [g]	After 100 brakes		After 200 brakes		After 300 brake	
		The weight of the pads after 100 braking [g]	Wear pads [g]	The weight of the pads after 100 braking [g]	Wear pads [g]	The weight of the pads after 100 braking [g]	Wear pads [g]
L	2766	2502	264	2217	285	1933	284
P	2751	2489	262	2202	287	1911	291
Σ			526	Σ	572	Σ	575

*L – left side, P – right side of the brake disc

[Own elaboration].

8. Conclusions

The article presents a proposal for a new segmented brake disk for rail vehicle wheels after testing according to PN EN 14535-3 and UIC 541-3. The brake disc, unlike the ones currently manufactured, was made in the welding technology of the friction plate with bars performing the function of both ventilation, positioning relative to the wheel and mounting to the wheel. The shield passed with a positive result, the test program included in the standard, there were no surface cracks or crushing of the target material for 1000 brakes in the strength test. In relation to the UIC card, the obtained values of instantaneous and average coefficient of friction are within the given tolerances for μ_a and μ_m , the temperature of the program disc B1 corresponding to the braking cases in the electric traction unit does not exceed 300°C (emergency braking). In terms of friction material wear, it was found that one set of organic friction linings allows for 300 braking. However, it should be emphasized that after this number of brakings, the thickness of linings remained 15 mm and the maximum per-

missible wear acc. UIC 541-3 cannot exceed 5 mm. Nonetheless, due to braking series of 100 brakes by PN EN 14535-3 in order not to repeat a given braking cycle due to the maximum wear of 5 mm that would occur during testing, the friction linings were replaced earlier.

Literature

1. Elektryczne zespoły trakcyjne, WWW http://www.pesa.pl/wp-content/uploads/2016/02/elektryczne_PL.pdf [access 26.04.19].
2. Karta UIC 541-3: Hamulec – Hamulec tarczowy i jego zastosowanie – Warunki dopuszczenia okładzin hamulcowych, 7 wydanie 2010, s. 12, 39.
3. PN-EN 14535-2: Kolejnictwo – tarcze hamulcowe kolejowych pojazdów szynowych – Część 2: Tarcze hamulcowe mocowane do kół, wymiary i wymagania dotyczące jakości, Warszawa 2011, s. 22.
4. PN-EN 14535-3: Kolejnictwo – Tarcze hamulcowe kolejowych pojazdów szynowych – Część 3: Tarcze hamulcowe, właściwości tarczy i pary ciernej, kła-

- syfikacja, Warszawa, 2016, s. 12–16.
5. Przybyszewski M.: *Elektryczne zespoły trakcyjne. Budowa, działanie, zasady utrzymania i obsługi*, Warszawa, Wydawnictwa Komunikacji i Łączności WKŁ, 2017, s. 66–69.
 6. Reibenschuh M. et.al.: *Modelling and Analysis of Thermal and Stress Loads in Train Disc Brakes – Braking from 250km/h to Standstill*, Journal of Mechanical Engineering 2009, pp. 55, 7–8, 494–502.
 7. Suwalski R., Zieliński A.: *Segmentowa tarcza hamulcowa typu 141BK do pojazdów kolejowych*, Problemy Kolejnictwa, 1994, nr 117, s. 89–104.
 8. Ścieszka S.F.: *Hamulce cierne. Zagadnienia materiałowe, konstrukcyjne i tribologiczne*, Wydawnictwo Gliwice – Radom, 1998.
 9. Tirović M.: *Energy thrift and improved performance achieved through novel railway brake discs*, Applied Energy 86 (2009) pp. 317–324.
 10. Wu S.C., Zhang S.Q., Xu Z.W.: *Thermal crack growth-based fatigue life prediction due to braking for a high-speed railway brake disc*, International Journal of Fatigue 87 (2016) pp. 359–369.

The project is financed by the National Centre for Research and Development, program LIDER V, agreement No. LIDER/022/359/L-5/13/NCBR/2014.